Wire Bonding UPH and Stitch Bond Improvement using 20 Micron Diameter Insulated Wire with Security Bump

Chunyan Nan[a*], Michael Mayer[a], Y. Norman Zhou[a], Jairus L. Pisigan[b], John Persic[b], Young-Kyu Song[b], and Henry Bathan[c]
[a] Centre for Advanced Materials Joining, University of Waterloo, Waterloo, ON N2L 3G1, Canada
Tel: 519-888-4024, FAX: 519-885-5862, [*]E-mail: cnan@uwaterloo.ca
[b] Microbonds Inc., Markham, ON L3R 3B3, Canada
Tel: 905-305-0980, FAX: 905-305-1078
[c] STATS ChipPAC, Singapore

Abstract

In this study, security bumps are used for strengthening the stitch bonds of two 20 micron diameter insulated Au wire bonding example processes. Bump bonding as a variant of the ball bonding process has been commonly used in the microelectronic industry to make bumps on dies that will later be flip-chip bonded. The optimized stitch bond parameters combined with the security bumps placed upon the stitch bonds substantially improve the second bond strength demonstrated on the two example processes on two different types of wire bonding equipment. A comparison of pull test results shows that security bumps increase stitch pull force up to 100%. The effect of varying the relative position (shift) of the security bump relative to the stitch bond location is investigated for one process. The window with the highest pull force improvement is ranging from 16 to 31 micron shift towards the ball bond. Looping with insulated wire is faster than with bare wire because of less effort to mitigate the risks of wires touching each other and producing a short. If two wire loops touch each other e.g. after molding, the wire insulation prevents shorts. Therefore, the looping requirements of the example processes with security bumps can be relaxed by reducing the number of kinks (reverses) from four to two. Due to the reduced looping complexity, the overall UPH increased with insulated wire by about 3.0 % and 4.9 % for the two processes, respectively. This increase is in spite of the time required for the additional security bumps, and compared to bare wire processes without security bumps but with more complex looping.

Key words: wire bonding, insulated wire, looping, security bump

1. Introduction

With the demands for increased circuit densities and finer pitches with improved reliability and accuracy in advanced microelectronic packaging, application of insulated bonding wire technology is attracting more attention [1]. Due to the insulating capability, wire touching, crossing, sagging, longer wires, and wire sweep can all be acceptable in mass production. This allows for more flexible package designs with improved performance and assembly yield e.g. for high-density packaging [2, 3]. Recent improvements of wire insulation technology increase wire coating purity and electrical flame off (EFO) consistency [4, 5]. A 25 µm gold wire with 0.5 µm thick coating for wire bonding application can achieve a breakdown strength of 200 V and an endurable baking temperature of 300 °C, without deterioration the wire strength or ball bondability [2]. Driven by demands for finer pitch interconnection and cost reduction, insulated wires with a reduced diameter of 20 µm are considered. To increase stitch bond quality and reliability for such wires, the use of security bumps formed on top of the stitch bonds is studied [6].

Several varieties of ball bumps are used in production, e.g. standard and stud bumps, bumps for stand-off stitch bonds (SSBs), and security bumps. A standard Au bump has the wire breaking within the heat affected zone (HAZ) as this is the weakest region of the wire. However, this type of bump can produce non-uniform tail length due to varying HAZ properties. A stud bump is formed by shearing the wire at the upper part of the bonded bump, producing a thin region where the tail can break [6], resulting in a more uniform tail length. Stacked stud bumps are used in flip chip packaging, increasing interconnect height to relieve stress [7, 8]. To improve bond reliability, bumps are used in chip-to-chip wire interconnects (SSB processes) [6], or as security bumps [9]. However, the bond speed is slowed down compared to standard bonding, due to the additional process steps for bump formation.

This paper investigates the application of security bumps to 20 µm insulated Au wire bonding processes in terms of bond strength and UPH. To compensate for the extra time needed for the security bump, the looping trajectory is simplified.

2. Experimental

Two studies (A and B) were carried out with different equipment, material and processes. Both studies had the goal of employing insulated wire without compromising on bond quality and throughput. Studies A and B were done at the University of Waterloo and STATS ChipPAC, respectively.

2.1 Study A

2.1.1 Materials

An ESEC 3100 automatic wirebonder (Esec, Cham, Switzerland) is used to perform thermosonic ball-stitch bonds, some followed by an in-process security bump. The substrate used is the diepad of a standard PLCC 44 leadframe with an 8 µm thick Ag metallization. A standard, bare Au bonding wire with a diameter of 20 µm and an insulated version of the same wire are used for the bonding tests (X-Wire™, Microbonds, Markham, ON). Table 1 shows the basic mechanical properties of the two wires.

Table 1 Wire properties at room temperature

Property	Insulated Wire[1]	Bare Wire[2]
Breaking Load [gf]	6.83-6.99	7.0-13.0
Elongation [%]	9.79-11.15	2.0-6.0

[1] actual measurements
[2] cited from wire specification

As Au wire bonds on Ag metallization are strong and reliable over the temperature range of 200-220 °C due to inexistence of intermetallic compounds or interface corrosion [1, 2], a bonding temperature of 220 °C is used for both the bare and insulated wire bonding process.

2.1.2 Stitch Bond Pull Force Optimization

The ultrasound time is 15 ms. To achieve improved bond quality using insulated wire, the stitch bond parameters of impact force (IF), bonding force (BF), and ultrasound (US) are optimized through a three-factor DOE method. The bonds are characterized by stitch bond pull force measurements. The process capability index (cpk) [3] is evaluated using

$$\text{cpk} = \frac{\mu - \text{LSL}}{3\sigma} \qquad \text{(Equation 1)}$$

where µ and σ are the PF average and standard deviation, and LSL is the lower specification limit LSL = 24 mN (2.45 gf).

In the 1st cycle of parameter optimization, the US value is varied from 30% to 60% in steps of 10%. Both the IF and BF are in the range of 200 mN to 600 mN, varied in steps of 100 mN. Two of the three variables are kept constant, the other is varied. From the results obtained with several different IF, BF, and US parameter combinations, the six combinations with the largest PF and cpk values are selected for the second cycle of optimization. These six combinations also allow for continuous bonding operation (no stoppages). An increased sample size of 20 bonds is used to obtain the average PF and cpk values given for the six combinations (test runs) in Table 2.

The parameters IF = 200 mN, BF = 300 mN, and US = 30% are used in test run 4 and result in the highest PF and cpk values in this study. They are selected as the optimized stitch bond parameters for process A.

2.1.3 The Formation of Security Bumps

After the formation of ball-stitch bonds, security bumps are immediately performed on top of the stitch bonds using the same bond material and temperature. To produce a consistent wire protrusion (tail) at the top of the bump, the bonder automatically shears the wire at the ball neck by a horizontal shift of the capillary, producing a stud bump. This shift is takes some time and is not required when using standard bumps. A schematic of the capillary movement during security bump formation is shown in Figure 1.

Table 2 Second cycle of stitch bond parameter optimization

Test Run	IF [mN]	BF [mN]	US [%]	Average PF [gf]	Stdev. PF [gf]	cpk
1	300	500	40	3.33	0.61	0.47
2	300	600	30	3.01	0.44	0.43
3	300	600	40	3.41	0.65	0.49
4	200	300	30	4.21	0.34	1.72
5	400	300	30	3.42	0.62	0.52
6	600	300	40	2.62	0.34	0.17

In Figures 1 (a)-(e), upon the formation of a ball bond on the substrate, the capillary rises to a predetermined vertical distance named 'separation height', followed by a movement across the ball neck to reduce wire connection, which is determined by the parameters of horizontal 'bump wedge distance' (BWD) and vertical 'bump height'. This shift of the capillary produces an annular inclined surface at the top of the ball bump. The capillary is then lift up with the wire clamp open to thread out the desired tail length. Then the clamp is closed to break the wire and leave a consistent tail protruding from the capillary tip. Table 3 shows the crucial parameters used to perform a robust and continuous stud bumping process.

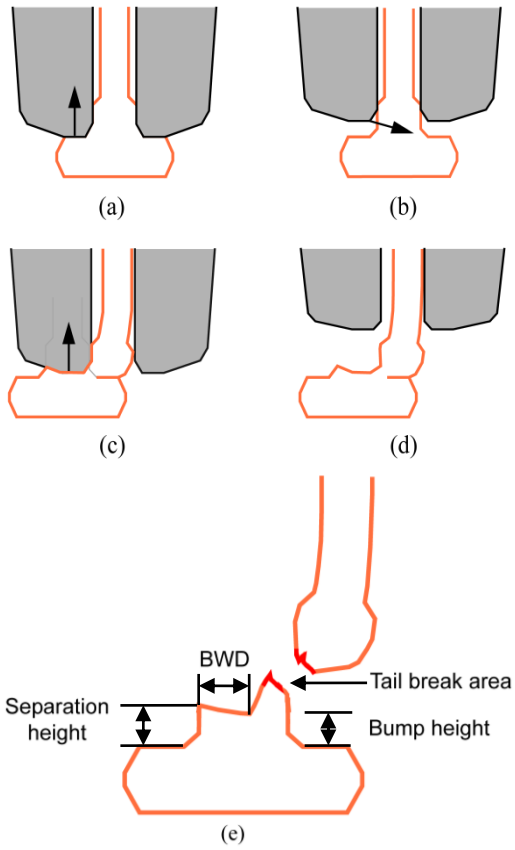

Fig.1 Schematic illustration of fundamental motions for stud bump formation as used for security bump. (a) Capillary moves upward after forming a ball bond; (b) capillary moves across the wire; (c) wire connection is reduced; (d) capillary lifts up and leaves a tail; (e) tail breaks. The "Bump Wedge Distance" (BWD) is one of the important process parameters.

Table 3 Key Parameters to Control Stud Bump

Parameter	Value
Bump Wedge Distance	12 µm
Bump Height	20 µm
Separation Height	25 µm

The position of the security bump relative to the preceding stitch bond is changed by varying the value of the 'wedge shift offset' (WSO) parameter. When WSO equals zero, the security bump is placed at the center of the stitch bond, i.e. in the center of the ring shaped imprint the capillary usually leaves on the substrate after a stitch bond. A negative value of WSO means the stitch bond is placed some distance away from the bump in the direction of the first bond. To strengthen the stitch bond, the bond areas of the bump and the stitch bond need to overlap. This is achieved by positive values of WSO, i.e. a shift of the stitch bond location away from the first bond location.

In the present study, a total of 200 security bumps are formed on top of stitch bonds using various bump locations (WSO between 0-31 µm). For WSO values of 32 µm and larger, undesired non-sticking of the bumps on the bonded wires and lift-offs of the stitch bonds are observed. The stitch bonds with security bumps are characterized by pull testing. The pull force results are compared with those of stitch bonds with comparable WSO values but without bump formation.

2.1.4 Loop Shaping

The trajectory required to form a desired wire loop shape with large enough accuracy has a large effect on production throughput and on the risk of electrical shorting. Loop shaping is a complex process which is influenced by multiple factors, including loop height, reverse loop trajectories that produce kinks, ball-wedge distance, formability of the wire and its HAZ, and others [10]. To meet the stringent requirements for fine pitch applications, loop shapes are characterized by multi reverse kinks. Loop profiles produced for this study with 2 kinks and 4 kinks are shown in Figure 2. Generally, it takes more time to form a loop with more kinks. Both, insulated and bare wires are used to assess the throughput [11] of processes with two or four loop kinks and with or without security bumps.

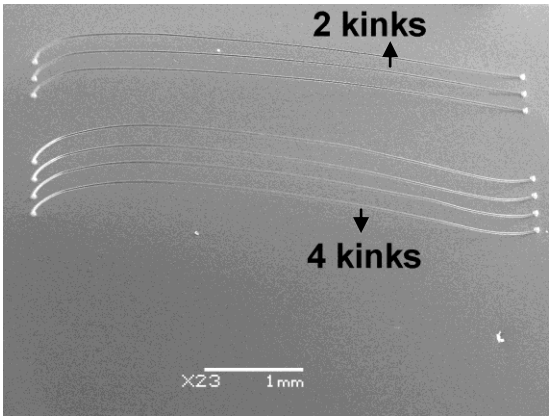

Fig. 2 Loop shapes formed using 2 and 4 reverse motions (kinks) with insulated wire.

2.2 Study B

A K&S Ultra automatic wirebonder (K&S, Fort Washington, USA) was used to perform thermosonic ball-stitch bonds, some followed by an in-process security bump. Similar 20 µm diameter Au wires were used as in study A. In particular, the insulated wire was a Tanaka GPG3 X-Wire™, and the bare wire was a Heraeus RelMax. An illustration of the bond material is schematically shown in Fig. 3.

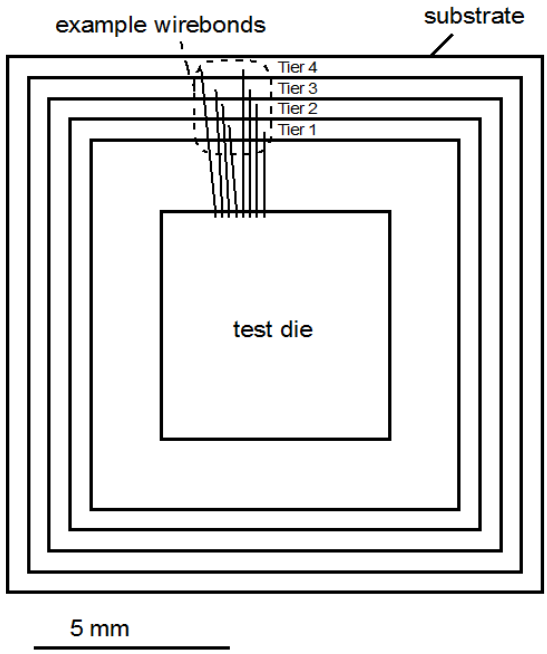

Fig. 3 Schematic of bond material after wire bonding (Study B). Bonds only schematic, not to scale, and may have different positions. Not all bonds are shown. Definition of substrate tiers.

Ball bonding was performed on peripheral pads on a test die with bond pad opening of 70 x 70 µm and a bond pad pitch of 85 µm. The stitch bonds were performed on Au/Pd/Ni plated 14x14 x0.75 QFN (2x2 matrix of 7x7mm) terminals of an organic substrate. The terminals are arranged in multiple tiers around the die. The four outer tiers are numbered 1-4 from inner to outer, and used for bonding. After bonding, the device had a total of 192 wire loops with lengths ranging from about 2.5 to 5 mm. A total of 16 wire loops were bonded on each of the two inner tiers, and 80 on each of the two outer tiers.

Generally, a two kink looping process was used for the bonds, except for the two outer tiers of some of the samples where a four kink looping process was used. A standard and two modified stitch bond processes were used. The standard process has one bond segment, the second process has two segments (pro-stitch), and the third process has one segment only but an added security bump.

The samples were molded after bonding using Hitachi mold compound. Five lots were produced with varying wire type and process parameters, as defined in Table 4.

In general, stitch bonds with insulated wire are expected to result in less PF than with bare wire unless the second bond is modified. The beneficial effect of such modifications is quantified. To this end, the comparison of lots 1 and 3 with lots 2 and 4 allows to determine the influence of adding a bond segment to the stitch bond process. The comparison of lost 1 and 3 with lot 5 allows to determine the influence of adding a security bump.

Modifying the stitch bond process reduces throughput. How much this reduction can be compensated by loop simplification is determined by comparing lot 1 with lot 4. How much the security bump related throughput reduction can be compensated by loop simplification is determined by comparing lot 1 with lot 5.

Table 4 Definition of Lots for Study B.

Lot#	Wire Type	Loop Kinks	Second Bond Process
1	bare	2-4	Standard
2	insulated	2-4	Pro-stitch
3	bare	2	Standard
4	insulated	2	Pro-stitch
5	insulated	2	Security Bump

3. Results and Discussion

3.1 Study A

3.1.1 Pull Strength for Various Bump Positions

SEM images of a ball bond (first bond) and a stitch bond with bump made with insulated wire are shown in Figs. 4 (a) and (b), respectively. Both the ball bond and the security bump present a typical 'watermelon' striping pattern at the ball surface. The dark areas represent coating material which has split during free air ball (FAB) formation [12]. This example security bump is located 28 µm from the stitch bond center towards the first bond.

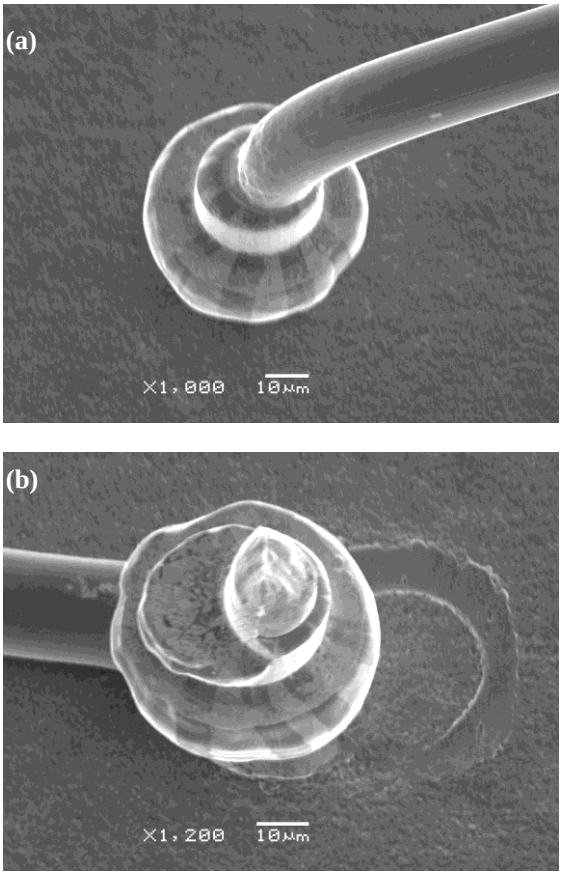

Fig. 4 SEM of insulated wire bonds (study A). Dark stripes on deformed ball is insulation layer. (a) Ball bond. (b) Stitch bond with security bump (WSO = 28 µm).

The pull force results of the stitch bonds with security bumps are shown in Fig. 5 for various WSO values. The x-symbols show the stitch bonds are lifted up at crescent bond area [13] during pull test, while the security bumps sit near the edge of the stitch bond. With increasing WSO, the stitch bond location moves towards that of the security bump, and the effective bond areas overlap. Enough overlap strengthens the stitch bonds causing wire break at the neck of the ball bonds during pull testing.

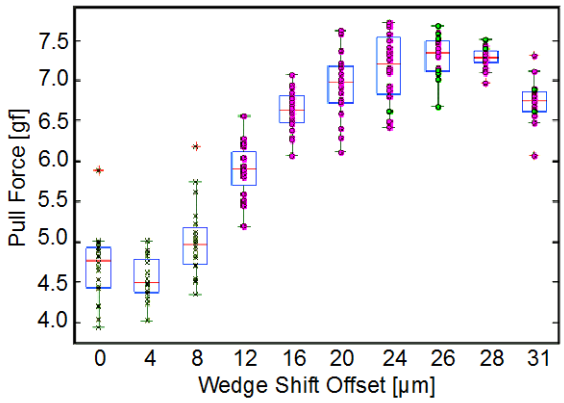

Fig. 5 Effect of bump position relative to stitch bond position on stitch pull strength with insulated wire. Pink circles: wire breaks at wire loop; green circles: wire breaks at ball neck; x-symbol: wire breaks at crescent bond area. Note the different step values on the horizontal axis.

When evaluating the data in Fig. 5, the optimal pull force values are found for WSO of 26 and 28 µm for average and cpk, respectively. For the WSO window between 16-31 µm, the PF is larger than 6 gf. The PF average ± standard deviation for this window is 7.01 ± 0.4 gf. Compared with the PF of stitch bonds without bump formation (4.21 ± 0.34 gf) from test run 4 in Table 2, the average PF is increased by 67% with security bumps.

3.1.2 Process Cycle Time

The various process cycle times are determined, shown in Fig. 6, and given in Table 5. A total of 15 ball-stitch bonds are performed at each condition. The cycle time does not depend on the wire type. The addition of security bumps results in process time increased by 58.0 ± 0.6 ms. The cycles with four kinks are 63.8 ± 1.1 ms longer than those with two kinks. This result depends on the type of looping and can vary substantially when adjusting looping parameters.

For devices with a large number of bonding wires, the UPH depends mainly on wire bond cycle time and less on pattern recognition for alignment and material indexing. For this work, UPH is assumed to be approximately proportional to the inverse of the

cycle time. With this assumption, the processes with security bumps and two kinks run at about 3 % higher UPH than those without security bump and with four kinks.

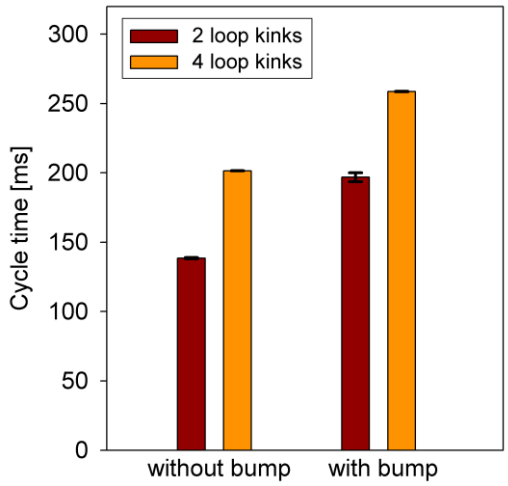

Fig. 6 Bond cycle time for various loop kinks and influence of security bump (study A).

Table 5 Evaluation of cycle times (Study A).

	Average cycle time [ms]			
	bare wire		insulated wire	
	2 kinks	4 kinks	2 kinks	4 kinks
without security bumps	138.5	201.5	137.8	202.0
with security bumps	196.9	258.7	195.1	261.4

3.2 Study B

The ball bond shape and shear strength of all lots are within typical specifications. The average loop heights (all lots, all tiers) range from 177 to 270 µm with standard deviations between 9 and 21 µm.

3.2.1 Stitch Bond Quality

The stitch PF results are given in Table 6. Generally, PF with bare wire and the standard process is largest (lots 1 and 3 compared to 2 and 4), even when using the two-segment stitch bonding process with insulated wire in this example. However, the PF with insulated wire and security bumps is substantially enhanced, amounting to 5.1 ± 0.4 gf, which is as large as that obtained with bare wire.

Table 6 Second Bond Characterization by Pull Test (Study B)

Statistics	Pull Force [gf]				
	Lot 1	Lot 2	Lot 3	Lot 4	Lot 5
Min	4.1	2.5	3.9	2.6	4.1
Ave	5.2	3.2	4.9	3.5	5.1
Max	5.9	4.2	5.7	4.6	5.7
Stdev	0.4	0.4	0.5	0.5	0.4

Optical micrographs of typical stitch bonds for each lot are given in Table 7. As expected, the bonds with the two segment process show an increased bond length. This is obvious when comparing the bond shapes of the bare wire lots (1 and 3, standard process) with the insulated wire lots (2 and 4, two segment process). Fractography of the pulled examples from the same lots indicates a somewhat larger fracture area of the bare wire bonds compared to the insulated. This could be the reason for the larger PF values with bare wire. For lot 5 (security bonds), the micrographs show the accurate placement of the bump, clearly overlapping and pinning down the stitch bond, assuring the increased PF. Observed pull modes for this lot include break at ball neck.

3.2.2 Bond UPH

The experimental UPH results are shown in Fig. 7. The highest UPH measured was UPH_M = 97.07 (lot 3). For the 192 wire device, this corresponds to a wire cycle time t_C of approximately

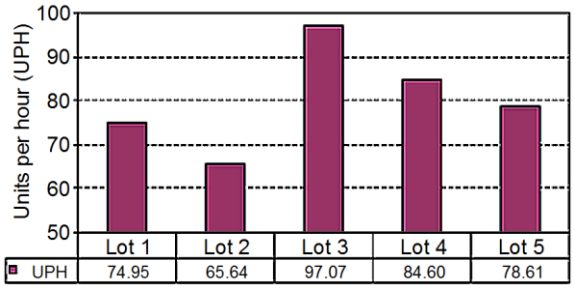

Fig. 7 Measured number of chips per hour (study B) completely wire bonded. A total of 192 bonded wire loops per chip.

Table 7 Micrographs of Example Stitch Bonds Before and After Pull Test (Study B).

Lot #	Bond loop direction							
	Southeast		Southwest		Northeast		Northwest	
	Before pull	After pull	Before pull	After pull	Before pull	After pull	Before pull	After pull
1	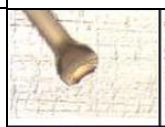					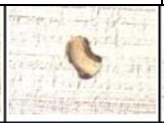		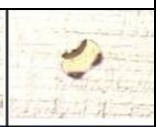
2			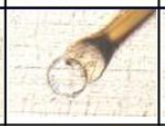					
3								
4	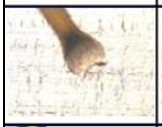							
5	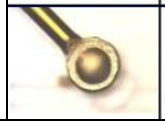		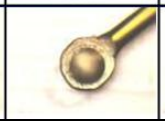					

$$t_C = \frac{3600}{n_W \cdot \mathrm{UPH_M}} = 193.2\ \mathrm{ms} \qquad \text{(Equation 2)}$$

where $n_W = 192$ is the number of wires per chip (unit). The value of t_C is different from those in study A due to the differences in the process requirements for the respective applications.

Replacing the standard stitch bond process with the two segment process reduces the UPH by an average of 10.9 or 13.5 %. The cycle time increases by an average of $\Delta t_C = 32.0$ ms. Lot 4 (only two kinks per loop) has a 64.0 ms shorter average cycle time than lot 1 (mix of wires with two and four kinks per loop). Therefore, the cycle time increase caused by the second segment can be completely compensated by loop simplification.

The addition of a security bump increases the cycle time by 45.4 ms (lot 5 compared to lot 3). However, loop simplification can completely compensate for this increase. The insulated wire process has an average cycle time of 238.5 ms (lot 5, security bump and loop simplification), which is 11.6 ms faster than the bare wire process requiring more complex looping (lot 1). This corresponds to a UPH improvement of 4.9 % if insulated wire is used instead of bare wire.

3.2.3 Wire Sway and Shorting After Molding

After compression molding the wire bonded chips, X-ray micrographs were taken and used to determine the amount of wire sway, defined by the maximum deviation of the loop location from the straight line between first and second bond, expressed in percent of the length of this straight line. A typical wire sway for lot 5 is 6.7 %. All other lots had similar or larger amounts of wire sway even if more kinks were used. Therefore, pinning the second bond with the security bond might have a beneficial influence on loop stability.

Electrical test were carried out to detect shorts between wire loops after molding. The results are shown in Fig. 9. In at least 5 % of the chips bonded with bare wire, shorts were detected. No shorts are detected within the insulated lots, indicating the efficient insulation in case of wires touching each other.

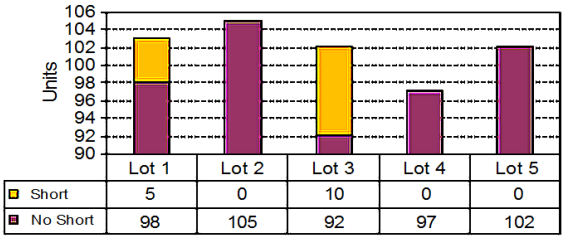

Fig. 9 Measured number of chips with and without electrical shorts. Study B.

4. Conclusions

A method is presented for using insulated bonding wire to improve UPH and avoid short by wire sway for a fine pitch wire bonding process without loss of bond quality. To achieve this, security bonds and simplified looping were applied.

The method is demonstrated in two different laboratories on different materials and equipment. This work adds to the growing amount of knowledge and guidelines of how to use insulated bonding wire technology in cases where enhanced process flexibility is required. The results serve as examples of how insulated wires can add value to wire bonding processes.

Acknowledgments

The authors would like to thank NSERC and IAMI for their financial support. The technical help of Esec USA is gratefully acknowledged.

References

[1] Z.W. Zhong, "Wire Bonding Using Insulated Wire and New Challenges in Wire Bonding", Microelectron. Int., vol. 25, no. 2, pp. 9-14, 2008.

[2] D. Lu, C. P. Wong, "Materials for Advanced Packaging", pp. 158-160, 2008.

[3] M. R. Ibrahim, A. T. K. Bee, "Bondability and Reliability for Insulated Wirebonding Process With 63 µm Pitch Capability", Proc. Electronics Packaging Technology Conf. (EPTC), vol. 1, 2005, pp. 283-286.

[4] C. Carr, J. Munar, W. Crockett, and R. Lyn, "Robust Wirebonding of X-Wire™ Insulated Bonding Wire Technology", Proc. IMAPS Symp., 2007, pp. 911-917.

[5] W. H. Song, C. Hang, and A. Pequegnat, "Comparison of Insulated with Bare Au Bonding Wire: HAZ Length, HAZ Breaking Force, and FAB Deformability", J. Electronic Materials, vol. 38, no. 6, 2009, pp. 834-42.

[6] G. Harman, "Wire Bonding in Microelectronics", McGraw Hill Professional, pp. 44-45, 164-166, 340-345, 2009.

[7] H. Liu, P. Niu, H. Hu, H. Chen, and Z. Xia, "A New Golden Bump Making Method for High Power LED Flip Chip", Proc. SPIE - The Int. Soc. Optical Engineering, vol. 6828, pp. 682810-1-8, 2007.

[8] T. Ogashiwa, T. Arikawa, H. Murai, A. Inoue, and T. Masumoto, "Reflowable Sn-Pb Bump Formation on Al Pad by a Solder Bumping Method", Proc. Electronic Compon. Technol. Conf. (ECTC), New York, NY: IEEE, pp. 1203-1208, 1995.

[9] M. Song, J. Yao, and Y. Lu, "Failure Mechanism and Solution Study of IC Wire Bond Heel Crack on Leadframe", Proc. Electronics Packaging Technol. Conf. (EPTC), pp. 1214-1219, 2008.

[10] S. K. Prasad, "Advanced Wirebond Interconnection Technology", Boston: Kluwer Academic Publishers, pp. 1-15, 2004.

[11] B. El-Haik, D. M. Roy, "Service design for six sigma: a roadmap for excellence", John Wiley and Sons, pp. 346-348, 2005.

[12] Susumu Okikawa, Michio Tanimoto, Hiroshi, Watanabe, Hiroshi, Mikino, and Tsuyoshi Kaneda, "Development of a Coated Wire Bonding Technology", IEEE Trans. Comp. Hybrids and Manuf. Tech. Vol. 12, No. 4. pp. 603-608, 1989.

[13] J. Lee, M. Mayer, Y. Zhou, S. J. Hong, and J. T. Moon, "Concurrent Optimization of Crescent Bond Pull Force and Tail Breaking Force in a Thermosonic Cu Wire Bonding Process", IEEE Trans. Electronics Packaging Manuf., vol. 32, no. 3, pp. 157-163, 2009.